Swansea University
Prifysgol Abertawe

Cronfa
Setting Research Free

Cronfa - Swansea University Open Access Repository

This is an author produced version of a paper published in :
Advanced Finite Element Technologies

Cronfa URL for this paper:
http://cronfa.swan.ac.uk/Record/cronfa28842

Book chapter :
Sevilla, R. & Huerta, A. (2016). *Tutorial on Hybridizable Discontinous Galerkin (HDG) for second-order elliptic problems.* Advanced Finite Element Technologies, (pp. 105-129). Springer International Publishing.
http://dx.doi.org/10.1007/978-3-319-31925-4_5

This article is brought to you by Swansea University. Any person downloading material is agreeing to abide by the terms of the repository licence. Authors are personally responsible for adhering to publisher restrictions or conditions. When uploading content they are required to comply with their publisher agreement and the SHERPA RoMEO database to judge whether or not it is copyright safe to add this version of the paper to this repository.
http://www.swansea.ac.uk/iss/researchsupport/cronfa-support/

Preprint of
Ruben Sevilla and Antonio Huerta. "Tutorial on Hybridizable Discontinuous Galerkin (HDG) for Second-Order Elliptic Problems."
Advanced Finite Element Technologies. Springer International Publishing, 2016. 105-129.

Tutorial on hybridizable discontinuous Galerkin (HDG) for second-order elliptic problems

Ruben Sevilla* and Antonio Huerta†

* Zienkiewicz Centre for Computational Engineering, College of Engineering, Swansea University, Bay Campus, SA1 8EN, Wales, United Kingdom
† Laboratori de Calcul Numeric (LaCaN). ETS de Ingenieros de Caminos, Canales y Puertos, Universitat Politecnica de Catalunya·BarcelonaTech, Barcelona, Spain

Abstract The HDG is a new class of discontinuous Galerkin (DG) methods that shares favorable properties with classical mixed methods such as the well known Raviart-Thomas methods. In particular, HDG provides optimal convergence of both the primal and the dual variables of the mixed formulation. This property enables the construction of superconvergent solutions, contrary to other popular DG methods. In addition, its reduced computational cost, compared to other DG methods, has made HDG an attractive alternative for solving problems governed by partial differential equations.

A tutorial on HDG for the numerical solution of second-order elliptic problems is presented. Particular emphasis is placed on providing all the necessary details for the implementation of HDG methods.

1 Introduction

Efficient and robust solution of equations of mathematical physics has been and still is a major concern for numerical analysts. In the last decades, discontinuous Galerkin (DG) techniques, originally introduced in Reed and Hill (1973), have become popular beyond their original applications in fluid dynamics or electromagnetic problems. DG methods provide a natural stabilization to the solution due to the inter-element fluxes. In recent years, hybrid DG methods have become more popular. According to Ciarlet (2002), a hybrid method is "any finite element method based on a formulation where one unknown is a function, or some of its derivatives, on the set Ω, and the other unknown is the trace of some of the derivatives of the same function, or the trace of the function itself, along the boundaries of the set". In fact,

Preprint of
Ruben Sevilla and Antonio Huerta. "Tutorial on Hybridizable Discontinuous Galerkin (HDG) for Second-Order Elliptic Problems."
Advanced Finite Element Technologies. Springer International Publishing, 2016. 105-129.

as noted by Arnold and Brezzi (1985), hybridization of DG methods derives from the mixed methods of Raviart and Thomas (1977), where the continuity constrain is eliminated from the finite element space and imposed by means of Lagrange multipliers on the inter-element boundaries. The idea was exploited by Cockburn and Gopalakrishnan (2004, 2005a,b) and Cockburn et al. (2009b) to formally develop the HDG method for second-order elliptic problems.

The HDG method is able to provide the optimal approximation properties that are characteristic of mixed methods, including the possibility to build a superconvergent solution, whilst retaining the advantages of DG methods. In addition, HDG methods are known to reduce the globally coupled degrees of freedom, when compared to other DG methods analyzed in Arnold et al. (2002). Recently, the comparisons between the HDG method and the traditional continuous Galerkin (CG) method, performed by Cockburn et al. (2009a) and Kirby et al. (2011), indicate that HDG methods are competitive, both in terms of the non-zero entries of the resulting matrix and the actual computing time. Huerta et al. (2013) evaluate the floating point operation counts for CG, DG and HDG schemes in 2D and 3D and for direct and iterative solvers. They conclude that HDG has comparable costs (in terms of floating point operations) to CG and that other advantages of HDG, such as block structured information and element-by-element operations, must be exploited to improve its performance compared to CG because parallelism and memory access are crucial for the final runtime. In fact, Yakovlev et al. (2015) compare CG and HDG from a practical perspective using the same object-oriented spectral element framework. They show that HDG can outperform the traditional CG approach when direct solvers for the linear system are used. Different conclusions are obtained when iterative solvers are employed, suggesting the need for tailormade preconditioners in an HDG framework. It is also worth emphasizing that the superconvergent properties of HDG enable the definition of efficient and inexpensive p-adaptive procedures not feasible in a standard CG approach, see for instance Giorgiani et al. (2013, 2014).

Since its introduction, the HDG has been objective of intensive research and has been applied to a large number of problems in different areas, including fluid mechanics (Nguyen et al., 2010, 2011a; Peraire et al., 2010), wave propagation (Nguyen et al., 2011c,b; Giorgiani et al., 2013) and solid mechanics (Soon et al., 2009; Kabaria et al., 2015), to name but a few.

This work presents a tutorial on the HDG method for the numerical solution of second-order elliptic problems. Section 2 presents the model second-order elliptic problem and its mixed formulation. The necessary notation is introduced in Section 3. The HDG method is presented in detail

Preprint of
Ruben Sevilla and Antonio Huerta. "Tutorial on Hybridizable Discontinuous Galerkin (HDG) for Second-Order Elliptic Problems."
Advanced Finite Element Technologies. Springer International Publishing, 2016. 105-129.

in Section 4, including the strong, weak and discrete forms and the corresponding equations. A new formulation, consisting on a variation of the standard HDG method is presented and its advantages are discussed. Special emphasis is placed on the computational aspects, providing an easy guide for the implementation of the HDG method. Additionally, numerical examples are used to illustrate the performance and the optimal approximation properties of the two HDG formulations. Section 5 presents the postprocessing technique that enables the computation of a superconvergent solution. Numerical examples are also included to show the benefits of the postprocessing technique and to illustrate its optimal approximation properties. Finally, Appendix A provides detailed expression of all the elemental matrices and vectors appearing in the discrete form of the HDG method.

2 Problem statement

Let $\Omega \in \mathbb{R}^{\mathtt{n_{sd}}}$ be an open bounded domain with boundary $\partial\Omega$ and $\mathtt{n_{sd}}$ the number of spatial dimensions. The strong form for the second-order elliptic problem can be written as

$$\begin{cases} -\boldsymbol{\nabla}\cdot\boldsymbol{\nabla}u = f & \text{in } \Omega, \\ u = u_D & \text{on } \Gamma_D, \\ \boldsymbol{n}\cdot\boldsymbol{\nabla}u = t & \text{on } \Gamma_N, \end{cases} \tag{1}$$

where $\partial\Omega = \overline{\Gamma}_D \cup \overline{\Gamma}_N$, $\overline{\Gamma}_D \cap \overline{\Gamma}_N = \emptyset$, $f \in \mathcal{L}_2(\Omega)$ is a source term and $\boldsymbol{n}$ is the outward unit normal vector to $\partial\Omega$. Note that standard Dirichlet and Neumann boundary conditions are considered. Of course, other mixed (i.e. Robin) boundary conditions can also be imposed but here, for clarity, they will not be detailed.

Moreover, assume that Ω is partitioned in $\mathtt{n_{el}}$ disjoint subdomains Ω_i

$$\overline{\Omega} = \bigcup_{i=1}^{\mathtt{n_{el}}} \overline{\Omega}_i, \quad \Omega_i \cap \Omega_j = \emptyset \text{ for } i \neq j,$$

with boundaries $\partial\Omega_i$, which define an internal interface Γ

$$\Gamma := \Big[\bigcup_{i=1}^{\mathtt{n_{el}}} \partial\Omega_i\Big] \setminus \partial\Omega \tag{2}$$

An equivalent strong form of the second-order elliptic problem can be

Preprint of
Ruben Sevilla and Antonio Huerta. "Tutorial on Hybridizable Discontinuous Galerkin (HDG) for Second-Order Elliptic Problems."
Advanced Finite Element Technologies. Springer International Publishing, 2016. 105-129.

written in the *broken* computational domain as

$$\begin{cases} -\boldsymbol{\nabla}\cdot\boldsymbol{\nabla}u = f & \text{in } \Omega_i, \text{ and for } i=1,\dots,\mathtt{n_{el}}, \\ u = u_D & \text{on } \Gamma_D, \\ \boldsymbol{n}\cdot\boldsymbol{\nabla}u = t & \text{on } \Gamma_N, \\ [\![u\boldsymbol{n}]\!] = \boldsymbol{0} & \text{on } \Gamma, \\ [\![\boldsymbol{n}\cdot\boldsymbol{\nabla}u]\!] = 0 & \text{on } \Gamma, \end{cases} \tag{3}$$

where the two last equations correspond to the imposition of the continuity of the primal variable u and the normal fluxes respectively along the internal interface Γ.

Note that the *jump* $[\![\cdot]\!]$ operator has been introduced following the definition by Montlaur et al. (2008). That is, along each portion of the interface Γ it sums the values from the left and right of say, Ω_i and Ω_j, namely

$$[\![\odot]\!] = \odot_i + \odot_j.$$

It is important to observe that this definition always requires the normal vector $\boldsymbol{n}$ in the argument and always produces functions in the same space as the argument.

Finally, the strong form is written in mixed form as a system of first order equations over the *broken* computational domain, namely

$$\begin{cases} \boldsymbol{\nabla}\cdot\boldsymbol{q} = f & \text{in } \Omega_i, \text{ and for } i=1,\dots,\mathtt{n_{el}}, \\ \boldsymbol{q}+\boldsymbol{\nabla}u = \boldsymbol{0} & \text{in } \Omega_i, \text{ and for } i=1,\dots,\mathtt{n_{el}}, \\ u = u_D & \text{on } \Gamma_D, \\ \boldsymbol{n}\cdot\boldsymbol{q} = -t & \text{on } \Gamma_N, \\ [\![u\boldsymbol{n}]\!] = \boldsymbol{0} & \text{on } \Gamma, \\ [\![\boldsymbol{n}\cdot\boldsymbol{q}]\!] = 0 & \text{on } \Gamma. \end{cases} \tag{4}$$

3 Functional and interpolation setting

In what follows, as usual, $(\cdot,\cdot)_D$ denotes the $\mathcal{L}_2$ scalar product in a generic subdomain D, that is

$$(u,v)_D = \int_D u\,v\,d\Omega \text{ and } (\boldsymbol{u},\boldsymbol{v})_D = \int_D \boldsymbol{u}\cdot\boldsymbol{v}\,d\Omega$$

for scalars and vectors respectively.

Preprint of
Ruben Sevilla and Antonio Huerta. "Tutorial on Hybridizable Discontinuous Galerkin (HDG) for Second-Order Elliptic Problems."
Advanced Finite Element Technologies. Springer International Publishing, 2016. 105-129.

Analogously, $< \cdot, \cdot >_S$ denotes the $\mathcal{L}_2$ scalar product in any domain $S \subset \Gamma \cup \partial\Omega$, that is

$$< u, v >_S = \int_S u\, v\, d\Gamma \text{ and } < \boldsymbol{u}, \boldsymbol{v} >_S = \int_S \boldsymbol{u} \cdot \boldsymbol{v}\, d\Gamma$$

for scalars and vectors respectively.

In the subsequent formulation the following scalar and vector spaces are used:

$$\begin{aligned} \boldsymbol{\mathcal{W}}(D) &= \{\boldsymbol{w} \in [\mathcal{H}^1(D)]^{\mathtt{n_{sd}}}, D \subseteq \Omega\}, \\ \mathcal{V}(D) &= \{v \in \mathcal{H}^1(D), D \subseteq \Omega\}, \\ \mathcal{M}(S) &= \{\mu \in \mathcal{L}_2(S), S \subseteq \Gamma \cup \partial\Omega\}. \end{aligned}$$

Moreover, the following discrete finite element spaces are introduced

$$\begin{aligned} \boldsymbol{\mathcal{W}}^h(\Omega) &= \{\boldsymbol{w} \in [\mathcal{L}_2(\Omega)]^{\mathtt{n_{sd}}}; \boldsymbol{w}|_{\Omega_i} \in [\mathcal{P}^p(\Omega_i)]^{\mathtt{n_{sd}}}\ \forall \Omega_i\} && \subset \boldsymbol{\mathcal{W}}(\Omega), \\ \mathcal{V}^h(\Omega) &= \{v \in \mathcal{L}_2(\Omega); v|_{\Omega_i} \in \mathcal{P}^p(\Omega_i)\ \forall \Omega_i\} && \subset \mathcal{V}(\Omega), \\ \mathcal{M}^h(S) &= \{\mu \in \mathcal{L}_2(S); \mu|_{\Gamma_i} \in \mathcal{P}^p(\Gamma_i)\ \forall \Gamma_i \subset S \subseteq \Gamma \cup \partial\Omega\} && \subset \mathcal{M}(S), \end{aligned}$$

where $\mathcal{P}^p(\Omega_i)$ and $\mathcal{P}^p(\Gamma_i)$ are the spaces of polynomial functions of degree at most $p \geq 1$ in Ω_i and Γ_i respectively. Note that $\mathcal{M}^h$ can be defined over all the mesh skeleton interior and exterior faces (or edges in two dimensions).

These spaces give rise to an element-by-element nodal interpolation of the corresponding variables, namely

$$\boldsymbol{q} \approx \boldsymbol{q}^h = \sum_{j=1}^{\mathtt{n_{en}}} N_j\, \mathbf{q}_j \qquad \in \boldsymbol{\mathcal{W}}^h, \tag{5a}$$

$$u \approx u^h = \sum_{j=1}^{\mathtt{n_{en}}} N_j\, \mathrm{u}_j \qquad \in \mathcal{V}^h, \tag{5b}$$

$$\hat{u} \approx \hat{u}^h = \sum_{j=1}^{\mathtt{n_{fn}}} \widehat{N}_j\, \hat{\mathrm{u}}_j \qquad \in \mathcal{M}^h(\Gamma \cup \Gamma_N) \text{ or } \mathcal{M}^h(\Gamma), \tag{5c}$$

where $\mathbf{q}_j$, u_j, and $\hat{\mathrm{u}}_j$ are nodal values, N_j are polynomial shape functions of order p in each element, $\mathtt{n_{en}}$ is the number of nodes per element, $\hat{N}_j$ are polynomial shape functions of order p in each element face/edge, and $\mathtt{n_{fn}}$ is the corresponding number of nodes per face/edge.

Given the element-by-element formulation, the vectors $\mathbf{u}_i$ and $\mathbf{q}_i$ are defined for each element $i = 1, \ldots, \mathtt{n_{el}}$. They include the corresponding nodal

Preprint of
Ruben Sevilla and Antonio Huerta. "Tutorial on Hybridizable Discontinuous Galerkin (HDG) for Second-Order Elliptic Problems."
Advanced Finite Element Technologies. Springer International Publishing, 2016. 105-129.

values described previously and are of dimension $\mathtt{n_{en}}$ and $\mathtt{n_{sd}n_{en}}$ respectively. The vector $\hat{\mathbf{u}}$ is defined globally over the mesh skeleton (faces/edges). Its dimension depends on the formulation and corresponds to the number of nodes on $\Gamma \cup \Gamma_N$ or on Γ. More precisely,

$$\dim(\hat{\mathbf{u}}) = \sum_{k=1}^{\mathtt{n_{ef}}} \mathtt{n}_{\mathtt{fn}}^{k},$$

where $\mathtt{n_{ef}}$ is the number of element faces/edges in the mesh skeleton and $\mathtt{n}_{\mathtt{fn}}^{k}$ is the number of nodes in the k-th face. The number of element faces/edges in the mesh skeleton always includes those on the interior, i.e. those belonging to Γ. But, depending on the formulation used, $\mathtt{n_{ef}}$ also includes the faces/edges on the Neumann boundary, Γ_N.

The HDG formulation solves problem (4) in two phases, see the seminal contribution by Cockburn et al. (2009b) and the subsequent papers by Cockburn et al. (2008) and Nguyen et al. (2009a,b, 2010, 2011a).

First, an element-by-element problem is defined with $(\boldsymbol{q}, u)$ as unknowns, and then a global problem is setup to determine the traces of u, denoted by $\hat{u}$, on the element boundaries. The local problem determines $\boldsymbol{q}_i := \boldsymbol{q}|_{\Omega_i}$ and $u_i := u|_{\Omega_i}$ for $i = 1, \dots, \mathtt{n_{el}}$ with a new variable $\hat{u}$ along the interface Γ acting as a Dirichlet boundary condition.

There are however several options for the detailed implementation. They are presented and discussed in the following sections.

4 The Hybridizable Discontinuous Galerkin

4.1 The strong forms

This is the classical formulation, it can be found in the series of papers by Nguyen et al. (2009a,b, 2010, 2011a) and rewrites (4) as two equivalent problems. First, the local —element-by-element— problem with Dirichlet boundary conditions is defined, namely

$$\begin{cases} \boldsymbol{\nabla} \cdot \boldsymbol{q}_i = f & \text{in } \Omega_i, \\ \boldsymbol{q}_i + \boldsymbol{\nabla} u_i = \mathbf{0} & \text{in } \Omega_i, \\ u_i = u_D & \text{on } \partial\Omega_i \cap \Gamma_D, \\ u_i = \hat{u} & \text{on } \partial\Omega_i \setminus \Gamma_D, \end{cases} \tag{6}$$

for $i = 1, \dots, \mathtt{n_{el}}$. Note that this approach assumes $\hat{u} \in \mathcal{L}_2(\Gamma \cup \Gamma_N)$ given. In each element Ω_i this problem produces an element-by-element solution $\boldsymbol{q}_i$ and u_i as a function of the unknown $\hat{u} \in \mathcal{L}_2(\Gamma \cup \Gamma_N)$. Note that these problems can be solved independently element by element.

Preprint of
Ruben Sevilla and Antonio Huerta. "Tutorial on Hybridizable Discontinuous Galerkin (HDG) for Second-Order Elliptic Problems."
Advanced Finite Element Technologies. Springer International Publishing, 2016. 105-129.

Second, a global problem is defined to determine $\hat{u}$. It corresponds to the imposition of the Neumann boundary condition and the so-called *transmission conditions*, see Cockburn et al. (2009b). These transmission conditions were already introduced in (4) to ensure inter-element continuity when the broken computational domain formulation was presented,

$$\begin{cases} [\![u\boldsymbol{n}]\!] = \boldsymbol{0} & \text{on } \Gamma, \\ [\![\boldsymbol{n}\cdot\boldsymbol{q}]\!] = 0 & \text{on } \Gamma, \\ \boldsymbol{n}\cdot\boldsymbol{q} = -t & \text{on } \Gamma_N. \end{cases}$$

Note that the first equation in the previous global problem imposes continuity of u along Γ. But $u = \hat{u}$ on Γ as imposed by the local problems (6). Hence, continuity of the primal variable, $[\![\hat{u}\boldsymbol{n}]\!] = \boldsymbol{0}$, is imposed automatically because $\hat{u}$ is unique for adjacent elements. In summary, the transmission conditions are simply

$$\begin{cases} [\![\boldsymbol{n}\cdot\boldsymbol{q}]\!] = 0 & \text{on } \Gamma, \\ \boldsymbol{n}\cdot\boldsymbol{q} = -t & \text{on } \Gamma_N. \end{cases} \tag{7}$$

4.2 The weak forms

The weak formulation for each element equivalent to (6) is as follows: for $i = 1, \dots, \mathtt{n_{el}}$, given u_D on Γ_D and $\hat{u}$ on $\Gamma \cup \Gamma_N$, find $(\boldsymbol{q}_i, u_i) \in \boldsymbol{\mathcal{W}}(\Omega_i) \times \mathcal{V}(\Omega_i)$ that satisfies

$$\begin{aligned} -(\boldsymbol{\nabla} v, \boldsymbol{q}_i)_{\Omega_i} + < v, \boldsymbol{n}_i \cdot \widehat{\boldsymbol{q}}_i >_{\partial\Omega_i} &= (v, f)_{\Omega_i} \\ -(\boldsymbol{w}, \boldsymbol{q}_i)_{\Omega_i} + (\boldsymbol{\nabla}\cdot\boldsymbol{w}, u_i)_{\Omega_i} &= < \boldsymbol{n}_i \cdot \boldsymbol{w}, u_D >_{\partial\Omega_i \cap \Gamma_D} + < \boldsymbol{n}_i \cdot \boldsymbol{w}, \hat{u} >_{\partial\Omega_i \setminus \Gamma_D}, \end{aligned}$$

for all $(\boldsymbol{w}, v) \in \boldsymbol{\mathcal{W}}(\Omega_i) \times \mathcal{V}(\Omega_i)$, where the numerical traces of the fluxes $\widehat{\boldsymbol{q}}_i$ must be defined. Note that this problem imposes the Dirichlet boundary conditions weakly.

The numerical traces of the fluxes are formally $\boldsymbol{n}_i \cdot \widehat{\boldsymbol{q}}_i = \boldsymbol{n}_i \cdot \boldsymbol{q}_i$ but, in practice, for stability, they are defined element-by-element (i.e. for $i = 1, \dots, \mathtt{n_{el}}$) as

$$\boldsymbol{n}_i \cdot \widehat{\boldsymbol{q}}_i := \begin{cases} \boldsymbol{n}_i \cdot \boldsymbol{q}_i + \tau_i (u_i - u_D) & \text{on } \partial\Omega_i \cap \Gamma_D, \\ \boldsymbol{n}_i \cdot \boldsymbol{q}_i + \tau_i (u_i - \hat{u}) & \text{elsewhere}, \end{cases} \tag{8}$$

with τ_i being a stabilization parameter defined element-by-element, whose selection has an important effect on the stability, accuracy and convergence properties of the resulting HDG method. The influence of the stabilization parameter has been studied extensively by Cockburn and co-workers, see for

Preprint of
Ruben Sevilla and Antonio Huerta. "Tutorial on Hybridizable Discontinuous Galerkin (HDG) for Second-Order Elliptic Problems."
Advanced Finite Element Technologies. Springer International Publishing, 2016. 105-129.

instance Cockburn et al. (2009b, 2008) and Nguyen et al. (2009a,b, 2010, 2011a). Choosing the correct stabilization parameter provides sufficient stabilization to the solution. Note that such a definition for the numerical trace is consistent, i.e. $\boldsymbol{n}_i \cdot \widehat{\boldsymbol{q}}_i = \boldsymbol{n}_i \cdot \boldsymbol{q}_i$ when $u_i = \hat{u}$ (and $u_i = u_D$). With the definition of the numerical fluxes given by (8), the weak problem becomes: for $i = 1, \dots, \mathtt{n_{el}}$, find $(\boldsymbol{q}_i, u_i) \in \boldsymbol{\mathcal{W}}(\Omega_i) \times \mathcal{V}(\Omega_i)$ that satisfies

$$\begin{aligned} &< v, \tau_i\, u_i >_{\partial\Omega_i} - (\boldsymbol{\nabla} v, \boldsymbol{q}_i)_{\Omega_i} + < v, \boldsymbol{n}_i \cdot \boldsymbol{q}_i >_{\partial\Omega_i} \\ &\qquad = (v, f)_{\Omega_i} + < v, \tau_i\, u_D >_{\partial\Omega_i \cap \Gamma_D} + < v, \tau_i\, \hat{u} >_{\partial\Omega_i \setminus \Gamma_D}, \end{aligned} \tag{9a}$$

$$\begin{aligned} &-(\boldsymbol{w}, \boldsymbol{q}_i)_{\Omega_i} + (\boldsymbol{\nabla} \cdot \boldsymbol{w}, u_i)_{\Omega_i} \\ &\qquad = < \boldsymbol{n}_i \cdot \boldsymbol{w}, u_D >_{\partial\Omega_i \cap \Gamma_D} + < \boldsymbol{n}_i \cdot \boldsymbol{w}, \hat{u} >_{\partial\Omega_i \setminus \Gamma_D}, \end{aligned} \tag{9b}$$

for all $(\boldsymbol{w}, v) \in \boldsymbol{\mathcal{W}}(\Omega_i) \times \mathcal{V}(\Omega_i)$. The weak form (9) for the *local problem* is equivalent to the strong form described by (6).

Once the weak form for the *local problem* is presented, the *global problem* (7) is of interest. The weak form equivalent to (7) is simply: find $\hat{u} \in \mathcal{M}(\Gamma \cup \Gamma_N)$ for all $\mu \in \mathcal{M}(\Gamma \cup \Gamma_N)$ such that

$$\sum_{i=1}^{\mathtt{n_{el}}} < \mu, \boldsymbol{n}_i \cdot \widehat{\boldsymbol{q}}_i >_{\partial\Omega_i \setminus \partial\Omega} + \sum_{i=1}^{\mathtt{n_{el}}} < \mu, \boldsymbol{n}_i \cdot \widehat{\boldsymbol{q}}_i + t >_{\partial\Omega_i \cap \Gamma_N} = 0,$$

where it is important to recall the definition of internal interface Γ given by (2).

Then, replacing (8) in the previous equation results in the global weak problem: find $\hat{u} \in \mathcal{M}(\Gamma \cup \Gamma_N)$ for all $\mu \in \mathcal{M}(\Gamma \cup \Gamma_N)$ such that

$$\begin{aligned} \sum_{i=1}^{\mathtt{n_{el}}} \Big\{ < \mu, \tau_i\, u_i >_{\partial\Omega_i \setminus \Gamma_D} + < \mu, \boldsymbol{n}_i \cdot \boldsymbol{q}_i >_{\partial\Omega_i \setminus \Gamma_D} - < \mu, \tau_i\, \hat{u} >_{\partial\Omega_i \setminus \Gamma_D} \Big\} \\ = - \sum_{i=1}^{\mathtt{n_{el}}} < \mu, t >_{\partial\Omega_i \cap \Gamma_N} . \end{aligned} \tag{10}$$

Note that both u_i and $\boldsymbol{q}_i$ are known functions of $\hat{u}$ once the local problems (9) are solved.

Remark 4.1 (Symmetric Dirichlet local problem)**.** There are two alternatives to symmetrize the local problem. The first one consists of integrating by parts the second term of the l.h.s. in (9a) leaving on the boundary of the element the values of the flux $\boldsymbol{q}_i$ in the interior. This strategy produces the

Preprint of
Ruben Sevilla and Antonio Huerta. "Tutorial on Hybridizable Discontinuous Galerkin (HDG) for Second-Order Elliptic Problems."
Advanced Finite Element Technologies. Springer International Publishing, 2016. 105-129.

following local problem:

$$\begin{aligned} &< v, \tau_i\, u_i >_{\partial\Omega_i} + (v, \boldsymbol{\nabla}\cdot\boldsymbol{q}_i)_{\Omega_i} \\ &\qquad = (v, f)_{\Omega_i} + < v, \tau_i\, u_D >_{\partial\Omega_i\cap\Gamma_D} + < v, \tau_i\, \hat{u} >_{\partial\Omega_i\setminus\Gamma_D}, \end{aligned} \tag{11a}$$

$$\begin{aligned} &(\boldsymbol{\nabla}\cdot\boldsymbol{w}, u_i)_{\Omega_i} - (\boldsymbol{w}, \boldsymbol{q}_i)_{\Omega_i} \\ &\qquad = < \boldsymbol{n}_i\cdot\boldsymbol{w}, u_D >_{\partial\Omega_i\cap\Gamma_D} + < \boldsymbol{n}_i\cdot\boldsymbol{w}, \hat{u} >_{\partial\Omega_i\setminus\Gamma_D}. \end{aligned} \tag{11b}$$

The second alternative consists of integrating by parts the second term on the l.h.s. of (9b) and change the sign of (9a), namely

$$\begin{aligned} &< v, \tau_i\, u_i >_{\partial\Omega_i} - (\boldsymbol{\nabla} v, \boldsymbol{q}_i)_{\Omega_i} + < v, \boldsymbol{n}_i\cdot\boldsymbol{q}_i >_{\partial\Omega_i} \\ &\qquad = (v, f)_{\Omega_i} + < v, \tau_i\, u_D >_{\partial\Omega_i\cap\Gamma_D} + < v, \tau_i\, \hat{u} >_{\partial\Omega_i\setminus\Gamma_D}, \\ &-(\boldsymbol{w}, \boldsymbol{\nabla} u_i)_{\Omega_i} + < \boldsymbol{n}_i\cdot\boldsymbol{w}, u >_{\partial\Omega_i} - (\boldsymbol{w}, \boldsymbol{q}_i)_{\Omega_i} \\ &\qquad = < \boldsymbol{n}_i\cdot\boldsymbol{w}, u_D >_{\partial\Omega_i\cap\Gamma_D} + < \boldsymbol{n}_i\cdot\boldsymbol{w}, \hat{u} >_{\partial\Omega_i\setminus\Gamma_D}. \end{aligned}$$

The first alternative is retained because it requires less computational effort (during the loop on faces/edges) than the second one.

4.3 The discrete forms and the corresponding equations

Section 3 introduced the necessary discrete spaces in order to prescribe the discrete weak forms for the local (11) and global (10) problems. The local problems are: for $i = 1, \dots \mathtt{n_{el}}$, find $(\boldsymbol{q}_i^h, u_i^h) \in \boldsymbol{\mathcal{W}}^h \times \mathcal{V}^h$ for all $(\boldsymbol{w}, v) \in \boldsymbol{\mathcal{W}}^h \times \mathcal{V}^h$ such that

$$\begin{aligned} &< v, \tau_i\, u_i^h >_{\partial\Omega_i} + (v, \boldsymbol{\nabla}\cdot\boldsymbol{q}_i^h)_{\Omega_i} \\ &\qquad = (v, f)_{\Omega_i} + < v, \tau_i\, u_D >_{\partial\Omega_i\cap\Gamma_D} + < v, \tau_i\, \hat{u}^h >_{\partial\Omega_i\setminus\Gamma_D}, \end{aligned} \tag{12a}$$

$$\begin{aligned} &(\boldsymbol{\nabla}\cdot\boldsymbol{w}, u_i^h)_{\Omega_i} - (\boldsymbol{w}, \boldsymbol{q}_i^h)_{\Omega_i} \\ &\qquad = < \boldsymbol{n}_i\cdot\boldsymbol{w}, u_D >_{\partial\Omega_i\cap\Gamma_D} + < \boldsymbol{n}_i\cdot\boldsymbol{w}, \hat{u}^h >_{\partial\Omega_i\setminus\Gamma_D}, \end{aligned} \tag{12b}$$

whereas the global problem is: find $\hat{u}^h \in \mathcal{M}^h(\Gamma\cup\Gamma_N)$ for all $\mu \in \mathcal{M}^h(\Gamma\cup\Gamma_N)$ such that

$$\begin{aligned} &\sum_{i=1}^{\mathtt{n_{el}}} \Big\{ < \mu, \tau_i\, u_i^h >_{\partial\Omega_i\setminus\Gamma_D} + < \mu, \boldsymbol{n}_i\cdot\boldsymbol{q}_i^h >_{\partial\Omega_i\setminus\Gamma_D} - < \mu, \tau_i\, \hat{u}^h >_{\partial\Omega_i\setminus\Gamma_D} \Big\} \\ &\qquad = -\sum_{i=1}^{\mathtt{n_{el}}} < \mu, t >_{\partial\Omega_i\cap\Gamma_N}. \end{aligned} \tag{13}$$

At this point, it is important to notice that (12) is well defined, see Theorem 4.2. Thus, with the interpolation chosen by (5), equations (12)

Preprint of
Ruben Sevilla and Antonio Huerta. "Tutorial on Hybridizable Discontinuous Galerkin (HDG) for Second-Order Elliptic Problems."
Advanced Finite Element Technologies. Springer International Publishing, 2016. 105-129.

give rise to the following system of equations for each element Ω_i (i.e., for $i = 1, \dots, \mathtt{n_{el}}$)

$$\begin{bmatrix} \mathbf{A}_{uu} & \mathbf{A}_{uq} \\ \mathbf{A}_{uq}^T & \mathbf{A}_{qq} \end{bmatrix}_i \begin{Bmatrix} \mathbf{u}_i \\ \mathbf{q}_i \end{Bmatrix} = \begin{Bmatrix} \mathbf{f}_u \\ \mathbf{f}_q \end{Bmatrix}_i + \begin{bmatrix} \mathbf{A}_{u\hat{u}} \\ \mathbf{A}_{q\hat{u}} \end{bmatrix}_i \hat{\mathbf{u}}_i. \tag{14a}$$

Recalling the dimensions of the different vectors presented in Section 3, this system requires inverting a dense matrix of dimension $(\mathtt{n_{sd}}+1)^2\mathtt{n_{en}}^2$.

Similarly, the interpolation defined by (5) applied to (13) produce the following system of equations

$$\sum_{i=1}^{\mathtt{n_{el}}} \left\{ \begin{bmatrix} \mathbf{A}_{u\hat{u}}^T & \mathbf{A}_{q\hat{u}}^T \end{bmatrix}_i \begin{Bmatrix} \mathbf{u}_i \\ \mathbf{q}_i \end{Bmatrix} + [\mathbf{A}_{\hat{u}\hat{u}}]_i \, \hat{\mathbf{u}}_i \right\} = \sum_{i=1}^{\mathtt{n_{el}}} [\mathbf{f}_{\hat{u}}]_i. \tag{14b}$$

A detailed description of the matrices and vectors appearing in (14) is given in Appendix A.

After replacing the solution of the local problem (14a) in (14b), the global problem becomes

$$\widehat{\mathbf{K}}\hat{\mathbf{u}} = \hat{\mathbf{f}}, \tag{15}$$

with

$$\widehat{\mathbf{K}} = \mathop{\mathbf{A}}_{i=1}^{\mathtt{n_{el}}} \begin{bmatrix} \mathbf{A}_{u\hat{u}}^T & \mathbf{A}_{q\hat{u}}^T \end{bmatrix}_i \begin{bmatrix} \mathbf{A}_{uu} & \mathbf{A}_{uq} \\ \mathbf{A}_{uq}^T & \mathbf{A}_{qq} \end{bmatrix}_i^{-1} \begin{bmatrix} \mathbf{A}_{u\hat{u}} \\ \mathbf{A}_{q\hat{u}} \end{bmatrix}_i + [\mathbf{A}_{\hat{u}\hat{u}}]_i \tag{16a}$$

and

$$\hat{\mathbf{f}} = \mathop{\mathbf{A}}_{i=1}^{\mathtt{n_{el}}} [\mathbf{f}_{\hat{u}}]_i - \begin{bmatrix} \mathbf{A}_{u\hat{u}}^T & \mathbf{A}_{q\hat{u}}^T \end{bmatrix}_i \begin{bmatrix} \mathbf{A}_{uu} & \mathbf{A}_{uq} \\ \mathbf{A}_{uq}^T & \mathbf{A}_{qq} \end{bmatrix}_i^{-1} \begin{Bmatrix} \mathbf{f}_u \\ \mathbf{f}_q \end{Bmatrix}_i. \tag{16b}$$

Note the symmetry of the (local and) global problem.

Theorem 4.2 (Well posedness of the local problem (Cockburn et al., 2009b))**.** *The local solver defined by* (12) *on* Ω_i *for each element* $i = 1, \dots, \mathtt{n_{el}}$ *is well defined if* $\tau_i > 0$ *on* $\partial\Omega_i$ *and* $\boldsymbol{\nabla}\mathcal{V}^h(\Omega_i) \subset \boldsymbol{\mathcal{W}}^h(\Omega_i)$

Proof. For homogeneous conditions, i.e. $\hat{u}^h = 0$, $f = 0$ and $u_D = 0$, and for $(\boldsymbol{w}, v) := (\boldsymbol{q}_i^h, u_i^h)$, equations (12) read

$$\begin{aligned} < u_i^h, \tau_i \, u_i^h >_{\partial\Omega_i} + (u_i^h, \boldsymbol{\nabla} \cdot \boldsymbol{q}_i^h)_{\Omega_i} &= 0, \\ (\boldsymbol{\nabla} \cdot \boldsymbol{q}_i^h, u_i^h)_{\Omega_i} - (\boldsymbol{q}_i^h, \boldsymbol{q}_i^h)_{\Omega_i} &= 0. \end{aligned}$$

Preprint of
Ruben Sevilla and Antonio Huerta. "Tutorial on Hybridizable Discontinuous Galerkin (HDG) for Second-Order Elliptic Problems."
Advanced Finite Element Technologies. Springer International Publishing, 2016. 105-129.

Hence, subtracting both equations

$$< u_i^h, \tau_i\, u_i^h >_{\partial\Omega_i} + (\boldsymbol{q}_i^h, \boldsymbol{q}_i^h)_{\Omega_i} = 0,$$

which implies, for $\tau_i > 0$ on $\partial\Omega_i$, that $\boldsymbol{q}_i^h = \mathbf{0}$ in Ω_i and $u_i^h = 0$ on $\partial\Omega_i$. Then, since $\boldsymbol{q}_i^h = \mathbf{0}$ in Ω_i equation (12b) becomes

$$(u_i^h, \boldsymbol{\nabla}\cdot\boldsymbol{w})_{\Omega_i} = 0 \quad \forall \boldsymbol{w} \in \boldsymbol{\mathcal{W}}^h$$

or, equivalently,

$$(\boldsymbol{\nabla} u_i^h, \boldsymbol{w})_{\Omega_i} = 0 \quad \forall \boldsymbol{w} \in \boldsymbol{\mathcal{W}}^h,$$

which implies $\boldsymbol{\nabla} u_i^h = \mathbf{0}$ in Ω_i and proves the result. □

Remark 4.3 (Computational aspect)**.** For implementation purposes, some auxiliary vectors are defined. As noticed by Theorem 4.2, problem (12) is well posed thus, equations (14a) can be solved and written as

$$\begin{Bmatrix} \mathbf{u}_i \\ \mathbf{q}_i \end{Bmatrix} = \begin{Bmatrix} \mathbf{z}_u^f \\ \mathbf{z}_q^f \end{Bmatrix}_i + \begin{bmatrix} \mathbf{Z}_u^{\hat{u}} \\ \mathbf{Z}_q^{\hat{u}} \end{bmatrix}_i \hat{\mathbf{u}}_i \tag{17}$$

where

$$\begin{Bmatrix} \mathbf{z}_u^f \\ \mathbf{z}_q^f \end{Bmatrix}_i = \begin{bmatrix} \mathbf{A}_{uu} & \mathbf{A}_{uq} \\ \mathbf{A}_{uq}^T & \mathbf{A}_{qq} \end{bmatrix}_i^{-1} \begin{Bmatrix} \mathbf{f}_u \\ \mathbf{f}_q \end{Bmatrix}_i \text{ and } \begin{bmatrix} \mathbf{Z}_u^{\hat{u}} \\ \mathbf{Z}_q^{\hat{u}} \end{bmatrix}_i = \begin{bmatrix} \mathbf{A}_{uu} & \mathbf{A}_{uq} \\ \mathbf{A}_{uq}^T & \mathbf{A}_{qq} \end{bmatrix}_i^{-1} \begin{bmatrix} \mathbf{A}_{u\hat{u}} \\ \mathbf{A}_{q\hat{u}} \end{bmatrix}_i$$

Then, (17) is replaced in (14b), which induces the same system of equations (15) but the matrix and vector defined by (16) are computed as follows:

$$\widehat{\mathbf{K}} = \mathop{\mathbf{A}}_{i=1}^{\mathtt{n_{el}}} \begin{bmatrix} \mathbf{A}_{u\hat{u}}^T & \mathbf{A}_{q\hat{u}}^T \end{bmatrix}_i \begin{bmatrix} \mathbf{Z}_u^{\hat{u}} \\ \mathbf{Z}_q^{\hat{u}} \end{bmatrix}_i + [\mathbf{A}_{\hat{u}\hat{u}}]_i \text{ and } \hat{\mathbf{f}} = \mathop{\mathbf{A}}_{i=1}^{\mathtt{n_{el}}} [\mathbf{f}_{\hat{u}}]_i - \begin{bmatrix} \mathbf{A}_{u\hat{u}}^T & \mathbf{A}_{q\hat{u}}^T \end{bmatrix}_i \begin{Bmatrix} \mathbf{z}_u^f \\ \mathbf{z}_q^f \end{Bmatrix}_i .$$

4.4 Numerical Example

In order to illustrate the results of HDG, the model problem (1) is solved in $\Omega :=]0,1[\times]0,1[$ with $\Gamma_N = \{(x,y) \in \partial\Omega \mid y = 0\}$ and $\Gamma_D = \partial\Omega \backslash \Gamma_N$. The source and boundary conditions are taken such that the analytical solution is given by

$$u(x,y) = 4y^2 - 4\lambda^2 y \exp(-\lambda y)\cos(6\pi x) + \lambda \exp(-2\lambda y),$$

where λ is a parameter that enables to control the strength of the solution gradient near the Neumann boundary. The effect of this parameter is illustrated in Figure 1, where the analytical solution is represented for two values of λ, namely 4 and 10.

Preprint of
Ruben Sevilla and Antonio Huerta. "Tutorial on Hybridizable Discontinuous Galerkin (HDG) for Second-Order Elliptic Problems."
Advanced Finite Element Technologies. Springer International Publishing, 2016. 105-129.

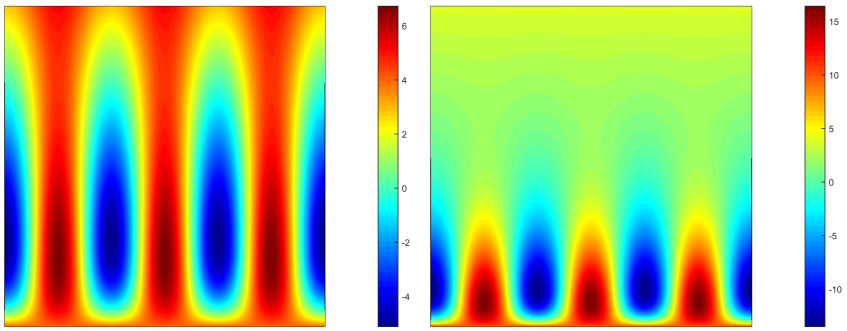

Figure 1. Model problem analytical solution: λ=4 (left) and λ=10 (right).

The first example involves the solution of the model problem with a value of λ=4. An extremely coarse mesh, with only eight elements, is considered, as shown in the left plot of Figure 2. The right plot of Figure 2 depicts the degrees of freedom used in an HDG computation with approximation order p=6. The black dots on the triangles denote the nodes used to build the polynomial approximation of the primal and dual solutions, u^h and $\boldsymbol{q}^h$ respectively. The red lines are the set of edges $\Gamma \cup \Gamma_N$ where the trace of the solution is approximated and the dots over these lines are the nodes used to build the polynomial approximation of $\hat{u}$. Note that there are no $\hat{u}^h$ unknowns along the Dirichlet boundary $\Gamma_D = \partial\Omega \backslash \Gamma_N$. The nodal distributions in elements and edges correspond to approximated optimal points presented in (Chen and Babuška, 1995) that are known to have better approximation properties than traditional equally-spaced nodal distributions.

The numerical solution computed with a polynomial approximation of degree p=6 is depicted in Figure 3, showing both the approximation of the solution in the element interiors and the approximation of the trace of the solution on $\Gamma \cup \Gamma_N$. It can be clearly observed that the numerical solution, u^h, is obviously discontinuous. More important, the numerical solution u^h and the numerical trace, $\hat{u}^h$, do not coincide on $\Gamma \cup \Gamma_N$ because the condition $u = \hat{u}$ in problem (6) is imposed in a weak sense.

Next, the model problem is considered with a value of λ=10. Figure 4 shows the numerical solution computed on a finer mesh, with 32 elements, and with a degree of approximation p=4 and p=5. It is worth noting how the jump of the solution on the element interfaces decreases as the degree of the approximation increases, suggesting the higher accuracy of the solution computed with p=5.

Preprint of
Ruben Sevilla and Antonio Huerta. "Tutorial on Hybridizable Discontinuous Galerkin (HDG) for Second-Order Elliptic Problems."
Advanced Finite Element Technologies. Springer International Publishing, 2016. 105-129.

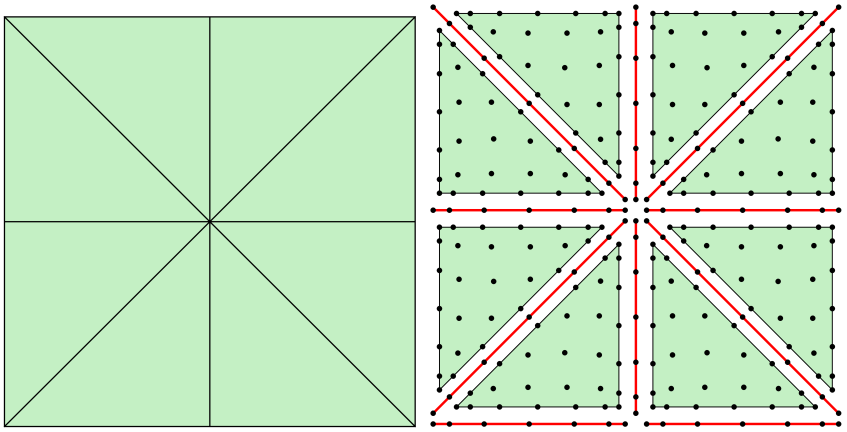

Figure 2. Coarse mesh of the domain Ω (left) and illustration of the degrees of freedom employed in an HDG computation with p=6 (right).

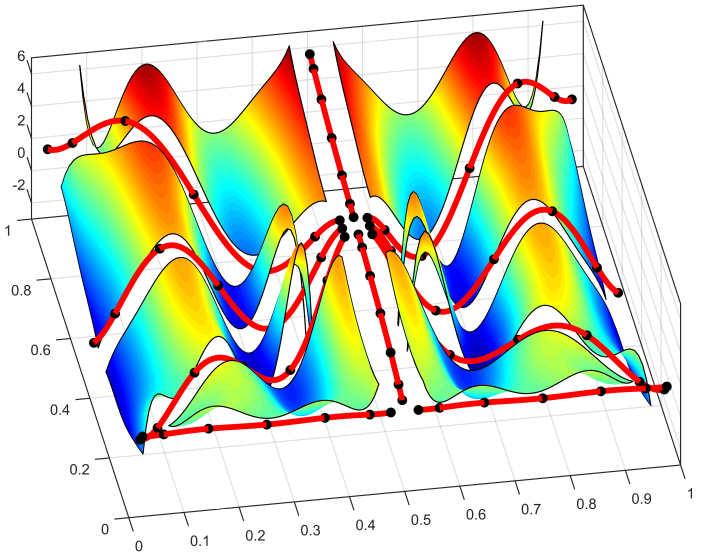

Figure 3. Model problem solution for p=6 on the mesh of Figure 2 showing both u^h in the element interiors and $\hat{u}^h$ on the edges $\Gamma \cup \Gamma_N$.

Preprint of
Ruben Sevilla and Antonio Huerta. "Tutorial on Hybridizable Discontinuous Galerkin (HDG) for Second-Order Elliptic Problems."
Advanced Finite Element Technologies. Springer International Publishing, 2016. 105-129.

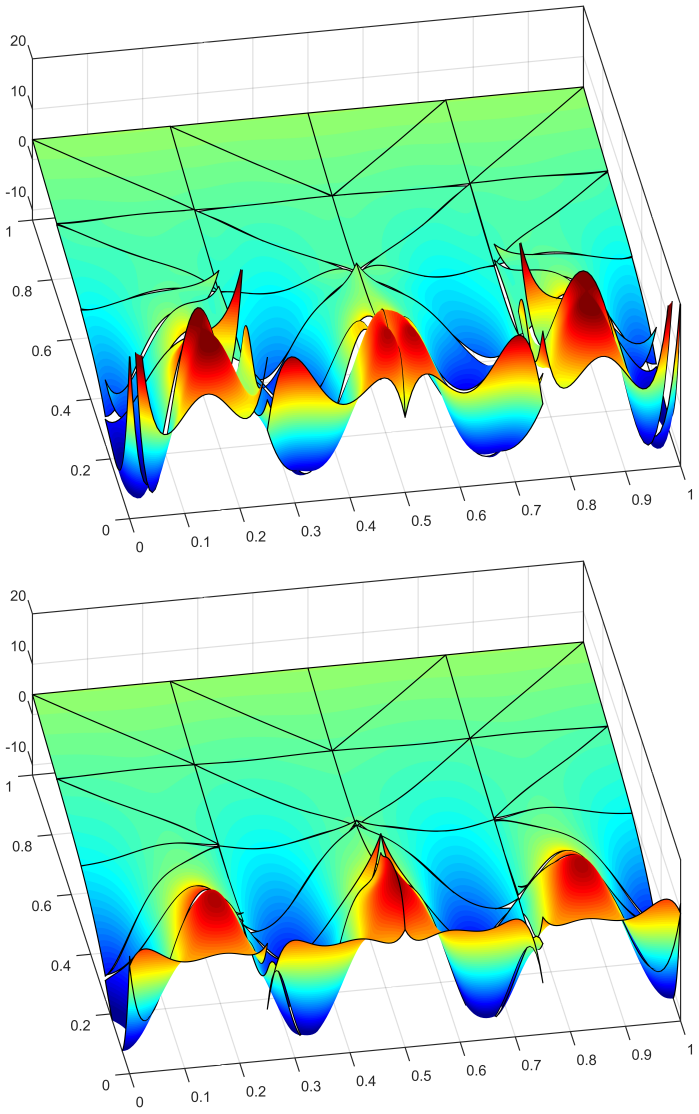

Figure 4. Model problem solution for p=4 (top) and p=5 (bottom) showing the improvement induced by an increase on the degree of approximation.

Preprint of
Ruben Sevilla and Antonio Huerta. "Tutorial on Hybridizable Discontinuous Galerkin (HDG) for Second-Order Elliptic Problems."
Advanced Finite Element Technologies. Springer International Publishing, 2016. 105-129.

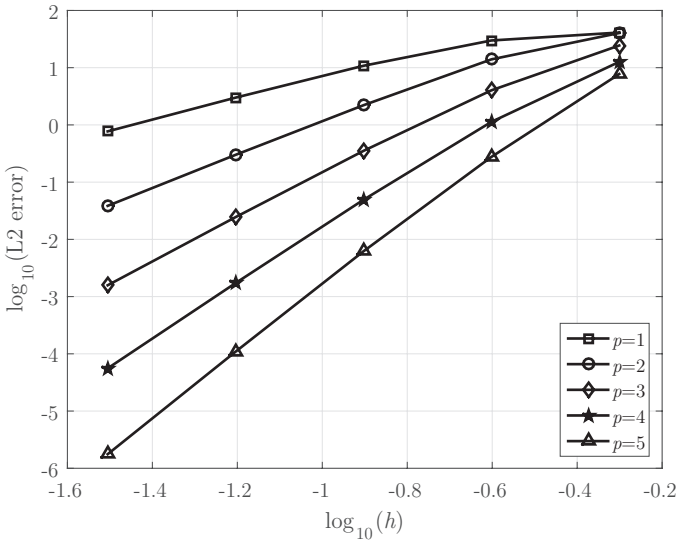

Figure 5. Error of u^h in the $\mathcal{L}_2(\Omega)$ norm as a function of the characteristic element size h for different values of the approximation degree p.

Finally, an h-convergence study is performed in order to check the optimal approximation properties of the implemented HDG formulation. Figure 5 shows the evolution of the error of u^h in the $\mathcal{L}_2(\Omega)$ norm as a function of the characteristic element size h for a degree of approximation p ranging from 1 to 5. For all the degrees of approximation considered, the optimal rate of convergence (i.e., p+1) is obtained. The results also illustrate the benefits of using high-order approximations. For instance, similar accuracy is obtained with a quartic approximation in a the mesh with 32 elements and with a linear approximation in a mesh with 2 048 elements. This implies that, in order to obtain a similar accuracy, linear elements require the solution of a system of equations ten times larger than the one induced by a quartic approximation.

4.5 Neumann local problems

A minor modification of the previous formulation can induce a smaller global problem. It consists of prescribing the Neumann boundary conditions already in the corresponding local problem. This modifies the original

Preprint of
Ruben Sevilla and Antonio Huerta. "Tutorial on Hybridizable Discontinuous Galerkin (HDG) for Second-Order Elliptic Problems."
Advanced Finite Element Technologies. Springer International Publishing, 2016. 105-129.

strong forms (6) and (7) as

$$\begin{cases} \boldsymbol{\nabla}\cdot\boldsymbol{q}_i = f & \text{in } \Omega_i, \\ \boldsymbol{q}_i + \boldsymbol{\nabla} u_i = \boldsymbol{0} & \text{in } \Omega_i, \\ u_i = u_D & \text{on } \partial\Omega_i \cap \Gamma_D, \\ \boldsymbol{n}_i\cdot\boldsymbol{q}_i = -t & \text{on } \partial\Omega_i \cap \Gamma_N, \\ u_i = \hat{u} & \text{on } \partial\Omega_i \setminus \partial\Omega, \end{cases} \tag{18}$$

for $i = 1, \dots \mathtt{n_{el}}$, and

$$[\![\boldsymbol{n}\cdot\boldsymbol{q}]\!] = 0 \text{ on } \Gamma. \tag{19}$$

It also implies a new definition for the numerical traces of the fluxes, thus (8) becomes, for $i = 1, \dots \mathtt{n_{el}}$,

$$\boldsymbol{n}_i\cdot\widehat{\boldsymbol{q}}_i := \begin{cases} \boldsymbol{n}_i\cdot\boldsymbol{q}_i + \tau_i(u_i - u_D) & \text{on } \partial\Omega_i\cap\Gamma_D, \\ \boldsymbol{n}_i\cdot\boldsymbol{q}_i + \tau_i(u_i - \hat{u}) & \text{on } \partial\Omega_i\cap\Gamma, \\ -t & \text{on } \partial\Omega_i\cap\Gamma_N. \end{cases} \tag{20}$$

Consequently, the weak form for the local problem, originally defined by (9) is now: for $i = 1, \dots \mathtt{n_{el}}$, find $(\boldsymbol{q}_i, u_i) \in \boldsymbol{\mathcal{W}}(\Omega_i)\times\mathcal{V}(\Omega_i)$ that satisfies

$$\begin{aligned} &< v, \tau_i\, u_i >_{\partial\Omega_i\setminus\Gamma_N} -(\boldsymbol{\nabla} v, \boldsymbol{q}_i)_{\Omega_i} + < v, \boldsymbol{n}_i\cdot\boldsymbol{q}_i >_{\partial\Omega_i\setminus\Gamma_N} \\ &\qquad = (v, f)_{\Omega_i} + < v, t >_{\partial\Omega_i\cap\Gamma_N} + < v, \tau_i\, u_D >_{\partial\Omega_i\cap\Gamma_D} \\ &\qquad\qquad + < v, \tau_i\, \hat{u} >_{\partial\Omega_i\setminus\partial\Omega}, \\ &-(\boldsymbol{w}, \boldsymbol{q}_i)_{\Omega_i} + (\boldsymbol{\nabla}\cdot\boldsymbol{w}, u_i)_{\Omega_i} - < \boldsymbol{n}\cdot\boldsymbol{w}, u_i >_{\partial\Omega_i\cap\Gamma_N} \\ &\qquad = < \boldsymbol{n}\cdot\boldsymbol{w}, u_D >_{\partial\Omega_i\cap\Gamma_D} + < \boldsymbol{n}\cdot\boldsymbol{w}, \hat{u} >_{\partial\Omega_i\setminus\partial\Omega}. \end{aligned}$$

for all $(\boldsymbol{w}, v) \in \boldsymbol{\mathcal{W}}(\Omega_i)\times\mathcal{V}(\Omega_i)$. To obtain the second equation above, it is important to recall that $\hat{u} \in \mathcal{L}_2(\Gamma)$ is not defined along Γ_N and, consequently, u_i is left along $\partial\Omega_i\cap\Gamma_N$. Following Remark 4.1, a symmetric version can also be obtained, namely

$$\begin{aligned} &< v, \tau_i\, u_i >_{\partial\Omega_i\setminus\Gamma_N} + (v, \boldsymbol{\nabla}\cdot\boldsymbol{q}_i)_{\Omega_i} - < v, \boldsymbol{n}_i\cdot\boldsymbol{q}_i >_{\partial\Omega_i\cap\Gamma_N} \\ &\qquad = (v, f)_{\Omega_i} + < v, t >_{\partial\Omega_i\cap\Gamma_N} + < v, \tau_i\, u_D >_{\partial\Omega_i\cap\Gamma_D} \\ &\qquad\qquad + < v, \tau_i\, \hat{u} >_{\partial\Omega_i\setminus\partial\Omega}, \end{aligned} \tag{21a}$$

$$\begin{aligned} &(\boldsymbol{\nabla}\cdot\boldsymbol{w}, u_i)_{\Omega_i} - < \boldsymbol{n}\cdot\boldsymbol{w}, u_i >_{\partial\Omega_i\cap\Gamma_N} -(\boldsymbol{w}, \boldsymbol{q}_i)_{\Omega_i} \\ &\qquad = < \boldsymbol{n}\cdot\boldsymbol{w}, u_D >_{\partial\Omega_i\cap\Gamma_D} + < \boldsymbol{n}\cdot\boldsymbol{w}, \hat{u} >_{\partial\Omega_i\setminus\partial\Omega}. \end{aligned} \tag{21b}$$

For the global problem, originally (10), continuity of fluxes is now only imposed along the internal faces, see (19). Hence, the global weak problem

Preprint of
Ruben Sevilla and Antonio Huerta. "Tutorial on Hybridizable Discontinuous Galerkin (HDG) for Second-Order Elliptic Problems."
Advanced Finite Element Technologies. Springer International Publishing, 2016. 105-129.

is: find $\hat{u} \in \mathcal{L}_2(\Gamma)$ for all $\mu \in \mathcal{L}_2(\Gamma)$ such that

$$\sum_{i=1}^{\mathtt{n_{el}}} < \mu, \left[\boldsymbol{n}_i \cdot \boldsymbol{q}_i + \tau(u_i - \hat{u})\right] >_{\partial\Omega_i \setminus \partial\Omega} = 0, \tag{22}$$

where the definition of the numerical flux, see (20), has already been used.

The discrete versions of these weak problem (21) and (22) are automatically determined as: for $i = 1, \dots \mathtt{n_{el}}$, find $(\boldsymbol{q}_i^h, u_i^h) \in \boldsymbol{\mathcal{W}}^h \times \mathcal{V}^h$ for all $(\boldsymbol{w}, v) \in \boldsymbol{\mathcal{W}}^h \times \mathcal{V}^h$ such that

$$\begin{aligned} < v, \tau_i\, u_i^h >_{\partial\Omega_i \setminus \Gamma_N} + (v, \boldsymbol{\nabla} \cdot \boldsymbol{q}_i^h)_{\Omega_i} - < v, \boldsymbol{n}_i \cdot \boldsymbol{q}_i^h >_{\partial\Omega_i \cap \Gamma_N} \\ = (v, f)_{\Omega_i} + < v, t >_{\partial\Omega_i \cap \Gamma_N} + < v, \tau_i\, u_D >_{\partial\Omega_i \cap \Gamma_D} \\ + < v, \tau_i\, \hat{u}^h >_{\partial\Omega_i \setminus \partial\Omega}, \end{aligned} \tag{23a}$$

$$\begin{aligned} (\boldsymbol{\nabla} \cdot \boldsymbol{w}, u_i^h)_{\Omega_i} - <\boldsymbol{n} \cdot \boldsymbol{w}, u_i^h >_{\partial\Omega_i \cap \Gamma_N} - (\boldsymbol{w}, \boldsymbol{q}_i^h)_{\Omega_i} \\ = < \boldsymbol{n} \cdot \boldsymbol{w}, u_D >_{\partial\Omega_i \cap \Gamma_D} + < \boldsymbol{n} \cdot \boldsymbol{w}, \hat{u}^h >_{\partial\Omega_i \setminus \partial\Omega}, \end{aligned} \tag{23b}$$

and find $\hat{u}^h \in \mathcal{M}^h(\Gamma)$ for all $\mu \in \mathcal{M}^h(\Gamma)$ such that

$$\sum_{i=1}^{\mathtt{n_{el}}} \left\{ <\mu, \tau\, u_i^h >_{\partial\Omega_i \setminus \partial\Omega} + <\mu, \boldsymbol{n}_i \cdot \boldsymbol{q}_i^h >_{\partial\Omega_i \setminus \partial\Omega} - <\mu, \tau\, \hat{u}^h >_{\partial\Omega_i \setminus \partial\Omega} \right\} = 0, \tag{24}$$

where, again, $(\boldsymbol{q}_i^h, u_i^h)$ are directly functions of $\hat{u}_i^h$ as determined by (23).

Finally, the following system of equations is obtained for the local problem, for each element $i = 1, \dots, \mathtt{n_{el}}$,

$$\begin{bmatrix} \mathbf{A}_{uu}^\star & \mathbf{A}_{uq}^\star \\ \mathbf{A}_{uq}^{\star T} & \mathbf{A}_{qq}^\star \end{bmatrix}_i \begin{Bmatrix} \mathbf{u}_i \\ \mathbf{q}_i \end{Bmatrix} = \begin{Bmatrix} \mathbf{f}_u^\star \\ \mathbf{f}_q \end{Bmatrix}_i + \begin{bmatrix} \mathbf{A}_{u\hat{u}}^\star \\ \mathbf{A}_{q\hat{u}}^\star \end{bmatrix}_i \hat{\mathbf{u}}_i. \tag{25a}$$

whereas the global system of equations is simply

$$\sum_{i=1}^{\mathtt{n_{el}}} \left\{ \begin{bmatrix} \mathbf{A}_{u\hat{u}}^{\star T} & \mathbf{A}_{q\hat{u}}^{\star T} \end{bmatrix}_i \begin{Bmatrix} \mathbf{u}_i \\ \mathbf{q}_i \end{Bmatrix} + [\mathbf{A}_{\hat{u}\hat{u}}^\star]_i\, \hat{\mathbf{u}}_i \right\} = 0. \tag{25b}$$

A detailed description of the matrices and vectors appearing in (25) is given in Appendix A.

The final global system, which retains all the symmetries, becomes

$$\widehat{\mathbf{K}}^\star \hat{\mathbf{u}} = \hat{\mathbf{f}}^\star, \tag{26a}$$

with

$$\widehat{\mathbf{K}}^\star = \mathop{\mathbf{A}}_{i=1}^{\mathtt{n_{el}}} \begin{bmatrix} \mathbf{A}_{u\hat{u}}^{\star T} & \mathbf{A}_{q\hat{u}}^{\star T} \end{bmatrix}_i \begin{bmatrix} \mathbf{A}_{uu}^\star & \mathbf{A}_{uq}^\star \\ \mathbf{A}_{uq}^{\star T} & \mathbf{A}_{qq}^\star \end{bmatrix}_i^{-1} \begin{bmatrix} \mathbf{A}_{u\hat{u}}^\star \\ \mathbf{A}_{q\hat{u}}^\star \end{bmatrix}_i + [\mathbf{A}_{\hat{u}\hat{u}}^\star]_i \tag{26b}$$

Preprint of
Ruben Sevilla and Antonio Huerta. "Tutorial on Hybridizable Discontinuous Galerkin (HDG) for Second-Order Elliptic Problems."
Advanced Finite Element Technologies. Springer International Publishing, 2016. 105-129.

and

$$\hat{\mathbf{f}}^\star = \mathop{\mathbf{A}}_{i=1}^{\mathtt{n_{el}}} - \begin{bmatrix}\mathbf{A}_{u\hat{u}}^{\star T} & \mathbf{A}_{q\hat{u}}^{\star T}\end{bmatrix}_i \begin{bmatrix}\mathbf{A}_{uu}^{\star} & \mathbf{A}_{uq}^{\star} \\ \mathbf{A}_{uq}^{\star T} & \mathbf{A}_{qq}\end{bmatrix}_i^{-1} \begin{Bmatrix}\mathbf{f}_u^\star \\ \mathbf{f}_q\end{Bmatrix}_i . \tag{26c}$$

Note that, in this case, the dimension of $\hat{\mathbf{u}}$ corresponds only to the degrees of freedom along the interior skeleton Γ, which is slightly smaller than in the previous case where unknowns had also to be determined along the Neumann boundary.

Theorem 4.4 (Well posedness of the local Neumann problem)**.** *The local solver defined by* (23) *on* Ω_i *for each element* $i = 1, \dots, \mathtt{n_{el}}$ *is well defined if* $\tau_i > 0$ *on* $\partial\Omega_i$ *and* $\boldsymbol{\nabla}\mathcal{V}^h(\Omega_i) \subset \boldsymbol{\mathcal{W}}^h(\Omega_i)$

Proof. For homogeneous conditions, i.e. $\hat{u}^h = 0$, $f = 0$ and $u_D = 0$, and for $(\boldsymbol{w}, v) := (\boldsymbol{q}_i^h, u_i^h)$, equations (23) read

$$< u_i^h, \tau_i\, u_i^h >_{\partial\Omega_i \setminus \Gamma_N} + (u_i^h, \boldsymbol{\nabla}\cdot\boldsymbol{q}_i^h)_{\Omega_i} - < u_i^h, \boldsymbol{n}_i \cdot \boldsymbol{q}_i^h >_{\partial\Omega_i \cap \Gamma_N} = 0, \tag{27}$$

$$(\boldsymbol{\nabla}\cdot\boldsymbol{q}_i^h, u_i^h)_{\Omega_i} - < \boldsymbol{n}\cdot\boldsymbol{q}_i^h, u_i^h >_{\partial\Omega_i \cap \Gamma_N} - (\boldsymbol{q}_i^h, \boldsymbol{q}_i^h)_{\Omega_i} = 0. \tag{28}$$

Hence, subtracting both equations

$$< u_i^h, \tau_i\, u_i^h >_{\partial\Omega_i \setminus \Gamma_N} + (\boldsymbol{q}_i^h, \boldsymbol{q}_i^h)_{\Omega_i} = 0,$$

which implies, for $\tau_i > 0$ on $\partial\Omega_i$, that $\boldsymbol{q}_i^h = \mathbf{0}$ in Ω_i and $u_i^h = 0$ on $\partial\Omega_i \setminus \Gamma_N$. Then, since $\boldsymbol{q}_i^h = \mathbf{0}$ in Ω_i equation (23b) becomes

$$(\boldsymbol{\nabla}\cdot\boldsymbol{w}, u_i^h)_{\Omega_i} - < \boldsymbol{n}\cdot\boldsymbol{w}, u_i^h >_{\partial\Omega_i \cap \Gamma_N} = 0 \quad \forall \boldsymbol{w} \in \boldsymbol{\mathcal{W}}^h$$

or, equivalently,

$$-(\boldsymbol{\nabla} u_i^h, \boldsymbol{w})_{\Omega_i} + < \boldsymbol{n}\cdot\boldsymbol{w}, u_i^h >_{\partial\Omega_i \setminus \Gamma_N} = 0 \quad \forall \boldsymbol{w} \in \boldsymbol{\mathcal{W}}^h.$$

But $u_i^h = 0$ on $\partial\Omega_i \setminus \Gamma_N$. Thus,

$$(\boldsymbol{\nabla} u_i^h, \boldsymbol{w})_{\Omega_i} = 0 \quad \forall \boldsymbol{w} \in \boldsymbol{\mathcal{W}}^h,$$

which implies $\boldsymbol{\nabla} u_i^h = \mathbf{0}$ in Ω_i and proves the result. □

4.6 Numerical Example

In order to illustrate the results of HDG by using the formulation with Neumann local problems, the model problem of Section 4.4 is considered with a value of λ=10. Figure 6 shows the numerical solution computed

Preprint of
Ruben Sevilla and Antonio Huerta. "Tutorial on Hybridizable Discontinuous Galerkin (HDG) for Second-Order Elliptic Problems."
Advanced Finite Element Technologies. Springer International Publishing, 2016. 105-129.

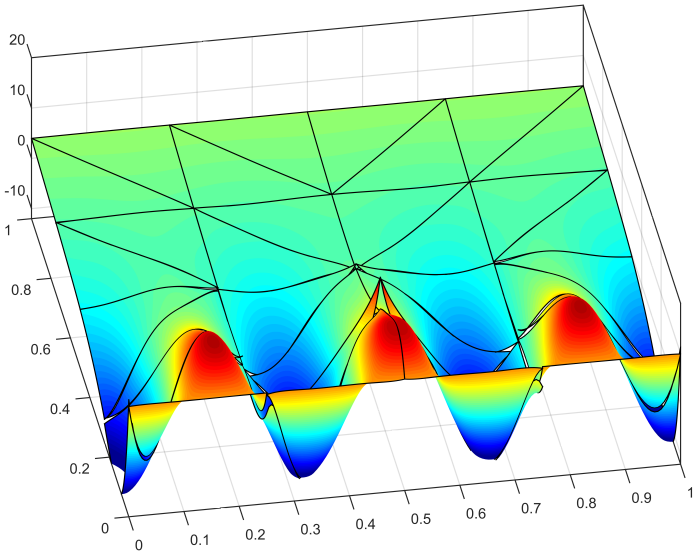

Figure 6. Model problem solution for p=5 using the formulation with Neumann local problems.

with a degree of approximation p=5. A visual comparison of the bottom plot in Figure 4 and Figure 6 suggests that the formulation with Neumann local problems provides a better accuracy of the solution near Neumann boundaries.

Next, an p-convergence study is performed in order to check the optimality of the approximation using the formulation with Neumann local problems and to compare the accuracy of the two HDG formulations considered in this work. Figure 7 shows the evolution of the error of u^h in the $\mathcal{L}_2(\Omega)$ norm as a function of the square root of the number of degrees of freedom of the global system of equations, i.e. $\mathtt{n_{dof}} = \dim(\hat{\mathbf{u}})$. Two meshes with 8 and 32 elements are considered and the degree of approximation is increased in each mesh from $p = 1$. The exponential rate of convergence is observed in all cases and the results reveal the advantage of using the formulation with Neumann local problems.

It is important to stress that the differences between the formulation with Dirichlet and Neumann local problems are noticed even if a global measure of the error is employed. Obviously, the extra accuracy provided by the formulation with Neumann problems is expected to be more relevant if the output of interest is defined near the Neumann boundary or on the

Preprint of
Ruben Sevilla and Antonio Huerta. "Tutorial on Hybridizable Discontinuous Galerkin (HDG) for Second-Order Elliptic Problems."
Advanced Finite Element Technologies. Springer International Publishing, 2016. 105-129.

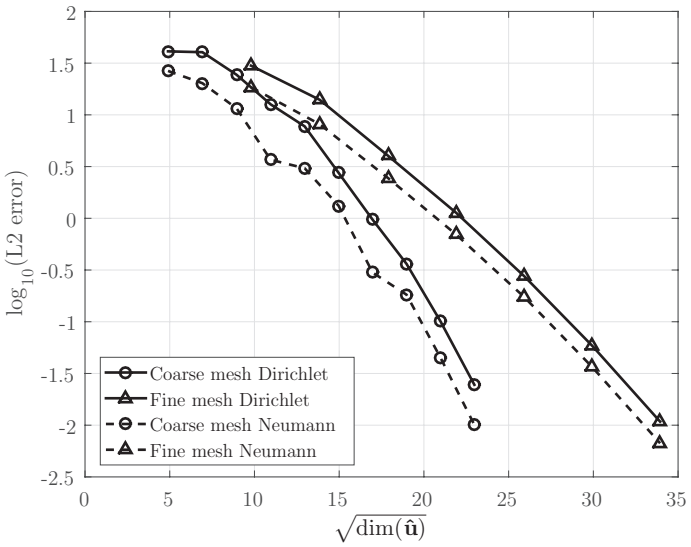

Figure 7. p-refinement: error of u^h for $p = 1, 2, 3, \ldots$ in the $\mathcal{L}_2(\Omega)$ norm as a function of $\sqrt{\text{dim}(\hat{\mathbf{u}})}$. The results are displayed for the HDG formulations with Dirichlet and Neumann local problems and for two different meshes.

Neumann boundary.

5 Postprocessed solution

The following well known a priori error estimate holds if a polynomial approximation of degree $p \geq 0$ is considered for the primal variable, u,

$$\|e_u\|_{\mathcal{L}_2(\Omega)} \leq C h^{p+1} |u|_{\mathcal{H}^{p+1}(\Omega)},$$

where e_u denotes the error of the primal variable, h is the characteristic mesh size and $\|\cdot\|$ and $|\cdot|$ denote the norm and the semi-norm, respectively, induced by the scalar product defined in Section 3, see for instance (Szabó and Babuška, 1991; Brenner and Scott, 1994).

Optimal convergence of the dual variable $\mathbf{q}$ is strongly dependent on the definition of the numerical flux. For a variety of DG methods, only convergence with order p was proved, see the unified analysis by Arnold et al. (2002). The first DG method with optimal convergence for the dual variable was introduced by Cockburn et al. (2009b). For a given element, assuming that the stabilisation parameter τ is equal to zero except on an

Preprint of
Ruben Sevilla and Antonio Huerta. "Tutorial on Hybridizable Discontinuous Galerkin (HDG) for Second-Order Elliptic Problems."
Advanced Finite Element Technologies. Springer International Publishing, 2016. 105-129.

arbitrary chosen element face, it was proved that the following a priori error estimate holds if a polynomial approximation of degree $p \geq 0$ is considered for the dual variable, $\mathbf{q}$,

$$\|e_{\mathbf{q}}\|_{\mathcal{L}_2(\Omega)} \leq Ch^{p+1}|\mathbf{q}|_{\mathcal{H}^{p+1}(\Omega)},$$

where $e_{\mathbf{q}}$ denotes the error of the dual variable, see Cockburn et al. (2008, 2009b,c) for more details.

Using the similarities of the HDG method and the Raviart-Thomas and Brezzi-Douglas-Marini mixed methods, see (Raviart and Thomas, 1977; Brezzi et al., 1985), it is possible to devise a *superconvergent* solution, $u_\star$, such that the following a priori error estimate holds

$$\|e_{u_\star}\|_{\mathcal{L}_2(\Omega)} \leq Ch^{p+2}|u|_{\mathcal{H}^{p+2}(\Omega)}.$$

for $p \geq 1$, see for instance (Cockburn et al., 2008, 2009b,c).

The postprocessed solution is computed by performing a postprocessing similar to the projection traditionally employed in the mixed method by Raviart and Thomas (1977), see also Arnold and Brezzi (1985). More precisely, the superconvergent postprocessed solution is obtained by solving the following problem in each element

$$\left\{\begin{array}{rcll} -\boldsymbol{\nabla}\cdot\boldsymbol{\nabla}u_\star & = & -\boldsymbol{\nabla}\cdot\mathbf{q}_h & \text{in } \Omega_i, \\ \boldsymbol{n}\cdot\boldsymbol{\nabla}u_\star & = & \boldsymbol{n}\cdot\mathbf{q}_h & \text{on } \partial\Omega_i, \end{array}\right. \tag{29}$$

with the additional solvability constraint

$$\int_{\Omega_i} u_\star = \int_{\Omega_i} u_h,$$

for $i = 1, \ldots, \mathtt{n_{el}}$.

If the approximation to the postprocessed solution, namely $u_\star^h$, is sought in a space $\mathcal{V}_\star^h(\Omega)$ that contains $\mathcal{V}^h(\Omega)$, asymptotic convergence of order $p+2$ can be proved, as shown by Cockburn et al. (2008). A typical choice for the richer space where $u_\star^h$ belongs is

$$\mathcal{V}_\star^h(\Omega) = \{v \in \mathcal{L}_2(\Omega); v|_{\Omega_i} \in \mathcal{P}^{p+1}(\Omega_i)\ \forall\Omega_i\}.$$

Figure 8 shows the postprocessed solution corresponding to an HDG computation with p=5 for the formulation with Neumann local problems. The gain in accuracy induced by the postprocessing is clearly observed by comparing the postprocessed solution in Figure 8 with the solution shown in Figure 6. In this example, the postprocessed solution $u_\star^h$ has an error in

Preprint of
Ruben Sevilla and Antonio Huerta. "Tutorial on Hybridizable Discontinuous Galerkin (HDG) for Second-Order Elliptic Problems."
Advanced Finite Element Technologies. Springer International Publishing, 2016. 105-129.

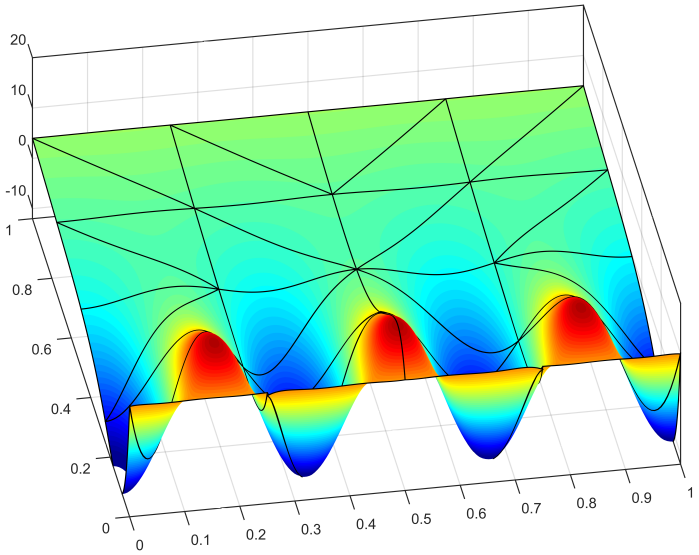

Figure 8. Model problem postprocessed solution for p=5 using the formulation with Neumann local problems.

the $\mathcal{L}_2(\Omega)$ norm, one order of magnitude lower than the error of the solution u^h.

It is important to remark that the significant extra accuracy provided by the postprocessing technique only requires the solution of the element-by-element problem (29), having a marginal cost compared to the cost of computing the solution u^h.

Next, an h-convergence study of the error of the postprocessed solution is performed. Figure 9 compares the evolution of the error of the solution u^h and the postprocessed solution $u^h_\star$ in the $\mathcal{L}_2(\Omega)$ norm as a function of the characteristic element size h and for a degree of approximation p ranging from 1 to 5. All the simulations correspond to the formulation with Neumann local problems.

The results show that the optimal (i.e., p+1 for the solution and p+2 for the post-processed solution) rate of convergence is obtained in all cases. The substantial gain in accuracy introduced by the postprocessing technique is clearly illustrated. As an example, the postprocessing of the solution computed in the finer mesh with $p = 5$ reduces the error by two orders of magnitude.

As expected, the same rate of convergence is obtained for the postpro-

Preprint of
Ruben Sevilla and Antonio Huerta. "Tutorial on Hybridizable Discontinuous Galerkin (HDG) for Second-Order Elliptic Problems."
Advanced Finite Element Technologies. Springer International Publishing, 2016. 105-129.

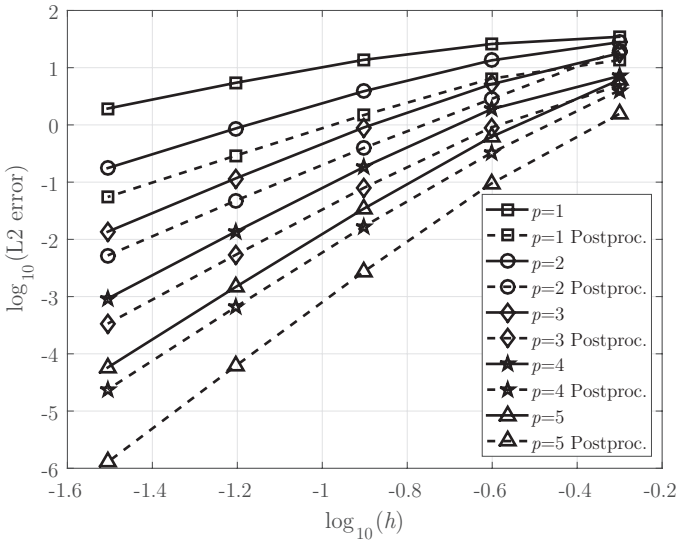

Figure 9. Error of the solution and the postprocessed solution in the $\mathcal{L}_2(\Omega)$ norm as a function of the characteristic element size h for different values of the approximation degree p.

cessed solution $u^h_\star$ that results from a computation with degree of approximation p and the solution u^h computed with a degree of approximation $p+1$. However, it is worth emphasizing that the postprocessed solution derived from a computation with degree of approximation p is always more accurate than the solution computed with a degree of approximation $p+1$. For instance, the postprocessed solution computed in the finer mesh with $p=4$ is two times more accurate than the solution computed in the finer mesh with $p=5$.

The extra accuracy of the postprocessed solution has been recently exploited by Giorgiani et al. (2013, 2014) to define a simple and inexpensive error estimator than can be used to develop highly efficient p-adaptive procedures.

Bibliography

D. N. Arnold and F. Brezzi. Mixed and nonconforming finite element methods: implementation, postprocessing and error estimates. *RAIRO Modél.*

Preprint of
Ruben Sevilla and Antonio Huerta. "Tutorial on Hybridizable Discontinuous Galerkin (HDG) for Second-Order Elliptic Problems."
Advanced Finite Element Technologies. Springer International Publishing, 2016. 105-129.

Math. Anal. Numér., 19(1):7–32, 1985.

D. N. Arnold, F. Brezzi, B. Cockburn, and L. D. Marini. Unified analysis of discontinuous Galerkin methods for elliptic problems. *SIAM J. Numer. Anal.*, 39(5):1749–1779, 2002.

S. C. Brenner and L. R. Scott. *The Mathematical Theory of Finite Element Methods*. Springer, 1994.

F. Brezzi, J. Douglas Jr, and L. D. Marini. Two families of mixed finite elements for second order elliptic problems. *Numer. Math.*, 47(2):217–235, 1985.

Q. Chen and I. Babuška. Approximate optimal points for polynomial interpolation of real functions in an interval and in a triangle. *Comput. Methods Appl. Mech. Eng.*, 128(3–4):405–417, 1995.

P. G. Ciarlet. *The finite element method for elliptic problems*, volume 40 of *Classics in Applied Mathematics*. Society for Industrial and Applied Mathematics (SIAM), Philadelphia, PA, 2002. Reprint of the 1978 original [North-Holland, Amsterdam].

B. Cockburn and J. Gopalakrishnan. A characterization of hybridized mixed methods for second order elliptic problems. *SIAM J. Numer. Anal.*, 42 (1):283–301, 2004.

B. Cockburn and J. Gopalakrishnan. Incompressible finite elements via hybridization. I. The Stokes system in two space dimensions. *SIAM J. Numer. Anal.*, 43(4):1627–1650, 2005a.

B. Cockburn and J. Gopalakrishnan. New hybridization techniques. *GAMM-Mitt.*, 28(2):154–182, 2005b.

B. Cockburn, B. Dong, and J. Guzmán. A superconvergent LDG-hybridizable Galerkin method for second-order elliptic problems. *Math. Comp.*, 77(264):1887–1916, 2008.

B. Cockburn, B. Dong, J. Guzmán, M. Restelli, and R. Sacco. A hybridizable discontinuous Galerkin method for steady-state convection-diffusion-reaction problems. *SIAM J. Sci. Comput.*, 31(5):3827–3846, 2009a.

B. Cockburn, J. Gopalakrishnan, and R. Lazarov. Unified hybridization of discontinuous Galerkin, mixed, and continuous Galerkin methods for second order elliptic problems. *SIAM J. Numer. Anal.*, 47(2):1319–1365, 2009b.

B. Cockburn, J. Guzmán, and H. Wang. Superconvergent discontinuous Galerkin methods for second-order elliptic problems. *Math. Comp.*, 78 (265):1–24, 2009c.

G. Giorgiani, S. Fernández-Méndez, and A. Huerta. Hybridizable discontinuous Galerkin p-adaptivity for wave propagation problems. *Int. J. Numer. Methods Fluids*, 72(12):1244–1262, 2013.

Preprint of
Ruben Sevilla and Antonio Huerta. "Tutorial on Hybridizable Discontinuous Galerkin (HDG) for Second-Order Elliptic Problems."
Advanced Finite Element Technologies. Springer International Publishing, 2016. 105-129.

G. Giorgiani, S. Fernández-Méndez, and A. Huerta. Hybridizable discontinuous Galerkin with degree adaptivity for the incompressible Navier–Stokes equations. *Comp. Fluids*, 98:196–208, 2014.

A. Huerta, A. Angeloski, X. Roca, and J. Peraire. Efficiency of high-order elements for continuous and discontinuous Galerkin methods. *Int. J. Numer. Methods Eng.*, 96(9):529–560, 2013.

H. Kabaria, A. J. Lew, and B. Cockburn. A hybridizable discontinuous Galerkin formulation for non-linear elasticity. *Comput. Methods Appl. Mech. Eng.*, 283:303–329, 2015.

R. Kirby, S. J. Sherwin, and B. Cockburn. To CG or to HDG: A comparative study. *J. Sci. Comput.*, 51(1):183–212, 2011.

A. Montlaur, S. Fernández-Méndez, and A. Huerta. Discontinuous Galerkin methods for the Stokes equations using divergence-free approximations. *Int. J. Numer. Methods Fluids*, 57(9):1071–1092, 2008.

N. Nguyen, J. Peraire, and B. Cockburn. A hybridizable discontinuous Galerkin method for Stokes flow. *Comput. Methods Appl. Mech. Eng.*, 199(9-12):582–597, 2010.

N. C. Nguyen, J. Peraire, and B. Cockburn. An implicit high-order hybridizable discontinuous Galerkin method for linear convection-diffusion equations. *J. Comput. Phys.*, 228(9):3232–3254, 2009a.

N. C. Nguyen, J. Peraire, and B. Cockburn. An implicit high-order hybridizable discontinuous Galerkin method for nonlinear convection-diffusion equations. *J. Comput. Phys.*, 228(23):8841–8855, 2009b.

N. C. Nguyen, J. Peraire, and B. Cockburn. An implicit high-order hybridizable discontinuous Galerkin method for the incompressible Navier-Stokes equations. *J. Comput. Phys.*, 230(4):1147–1170, 2011a.

N. C. Nguyen, J. Peraire, and B. Cockburn. High-order implicit hybridizable discontinuous Galerkin methods for acoustics and elastodynamics. *J. Comput. Phys.*, 230(10):3695–3718, 2011b.

N. C. Nguyen, J. Peraire, and B. Cockburn. Hybridizable discontinuous Galerkin methods for the time-harmonic Maxwell's equations. *J. Comput. Phys.*, 230(19):7151–7175, 2011c.

J. Peraire, N. Nguyen, and B. Cockburn. A hybridizable discontinuous Galerkin method for the compressible Euler and Navier-Stokes equations. *AIAA paper*, 363:2010, 2010.

P.-A. Raviart and J. M. Thomas. A mixed finite element method for 2nd order elliptic problems. In *Mathematical aspects of finite element methods (Proc. Conf., Consiglio Naz. delle Ricerche (C.N.R.), Rome, 1975)*, pages 292–315. Lecture Notes in Math., Vol. 606. Springer, Berlin, 1977.

W. Reed and T. Hill. Triangular mesh methods for the neutron transport equation. Technical report, Los Alamos Scientific Laboratory, 1973.

Preprint of
Ruben Sevilla and Antonio Huerta. "Tutorial on Hybridizable Discontinuous Galerkin (HDG) for Second-Order Elliptic Problems."
Advanced Finite Element Technologies. Springer International Publishing, 2016. 105-129.

S.-C. Soon, B. Cockburn, and H. K. Stolarski. A hybridizable discontinuous Galerkin method for linear elasticity. *Int. J. Numer. Methods Eng.*, 80 (8):1058–1092, 2009.

B. Szabó and I. Babuška. *Finite Element Analysis*. John Wiley & Sons, New York, 1991.

F. D. Witherden and P. E. Vincent. On the identification of symmetric quadrature rules for finite element methods. *Comput. Math. Appl.*, 69 (10):1232–1241, 2015.

S. Yakovlev, D. Moxey, R. M. Kirby, and S. J. Sherwin. To CG or to HDG: A comparative study in 3D. *J. Sci. Comput.*, pages 1–29, 2015.

A Implementation details

This appendix is devoted to the detailed presentation of the matrices and vectors appearing in the discrete version of both the local and global problems induced by the HDG method.

The interpolation functions and their derivatives, used in (5), are defined in a reference element, with local coordinates $\boldsymbol{\xi}$. The isoparametric transformation is used to relate local and Cartesian coordinates, namely

$$\boldsymbol{x}(\boldsymbol{\xi}) = \sum_{i=1}^{\mathtt{n_{en}}} \boldsymbol{x}_i \mathbf{N}_i(\boldsymbol{\xi}),$$

where $\boldsymbol{x}_i$ denote the elemental nodal coordinates.

The following compact form of the interpolation functions is introduced

$$\mathbf{N} = \begin{bmatrix} N_1 & N_2 & \dots & N_{\mathtt{n_{en}}} \end{bmatrix}^T, \quad \widehat{\mathbf{N}} = \begin{bmatrix} \widehat{N}_1 & \widehat{N}_2 & \dots & \widehat{N}_{\mathtt{n_{fn}}} \end{bmatrix}^T,$$

$$\mathbf{N}_{\boldsymbol{n}} = \begin{bmatrix} N_1\boldsymbol{n} & N_2\boldsymbol{n} & \dots & N_{\mathtt{n_{en}}}\boldsymbol{n} \end{bmatrix}^T, \quad \widehat{\mathbf{N}}_{\boldsymbol{n}} = \begin{bmatrix} \widehat{N}_1\boldsymbol{n} & \widehat{N}_2\boldsymbol{n} & \dots & \widehat{N}_{\mathtt{n_{fn}}}\boldsymbol{n} \end{bmatrix}^T,$$

$$\boldsymbol{\nabla}\mathbf{N} = \begin{bmatrix} \left(\boldsymbol{J}^{-1}\boldsymbol{\nabla}N_1\right)^T & \left(\boldsymbol{J}^{-1}\boldsymbol{\nabla}N_2\right)^T & \dots & \left(\boldsymbol{J}^{-1}\boldsymbol{\nabla}N_{\mathtt{n_{en}}}\right)^T \end{bmatrix}^T,$$

$$\mathbf{N}_{\mathtt{n_{sd}}} = \begin{bmatrix} N_1\boldsymbol{I}_{\mathtt{n_{sd}}} & N_2\boldsymbol{I}_{\mathtt{n_{sd}}} & \dots & N_{\mathtt{n_{en}}}\boldsymbol{I}_{\mathtt{n_{sd}}} \end{bmatrix}^T,$$

where $\boldsymbol{n} = (n_1, \dots, n_{\mathtt{n_{sd}}})$ denotes the outward unit normal vector to an edge/face, $\boldsymbol{J}$ is the Jacobian of the isoparametric transformation and $\boldsymbol{I}_{\mathtt{n_{sd}}}$ is the identity matrix of dimension $\mathtt{n_{sd}}$.

The different matrices appearing in (14), computed for each element $i = 1, \dots, \mathtt{n_{el}}$, can be expressed as

$$[\mathbf{A}_{uu}]_i = \sum_{\partial\Omega_i} \tau_i \sum_{\mathtt{g}=1}^{\mathtt{n_{ip}^f}} \mathbf{N}(\boldsymbol{\xi}_{\mathtt{g}}^{\mathtt{f}})\, \mathbf{N}^T(\boldsymbol{\xi}_{\mathtt{g}}^{\mathtt{f}}) w_{\mathtt{g}}^{\mathtt{f}},$$

Preprint of
Ruben Sevilla and Antonio Huerta. "Tutorial on Hybridizable Discontinuous Galerkin (HDG) for Second-Order Elliptic Problems."
Advanced Finite Element Technologies. Springer International Publishing, 2016. 105-129.

$$[\mathbf{A}_{qq}]_i = -\sum_{\mathtt{g}=1}^{\mathtt{n}^{\mathtt{e}}_{\mathtt{ip}}} \mathbf{N}_{\mathtt{n}_{\mathtt{sd}}}(\boldsymbol{\xi}^{\mathtt{e}}_{\mathtt{g}})\, \mathbf{N}^T_{\mathtt{n}_{\mathtt{sd}}}(\boldsymbol{\xi}^{\mathtt{e}}_{\mathtt{g}}) w^{\mathtt{e}}_{\mathtt{g}},$$

$$[\mathbf{A}_{uq}]_i = \sum_{\mathtt{g}=1}^{\mathtt{n}^{\mathtt{e}}_{\mathtt{ip}}} \mathbf{N}(\boldsymbol{\xi}^{\mathtt{e}}_{\mathtt{g}})\, \boldsymbol{\nabla}\mathbf{N}^T(\boldsymbol{\xi}^{\mathtt{e}}_{\mathtt{g}}) w^{\mathtt{e}}_{\mathtt{g}},$$

$$[\mathbf{f}_u]_i = \sum_{\mathtt{g}=1}^{\mathtt{n}^{\mathtt{e}}_{\mathtt{ip}}} \mathbf{N}(\boldsymbol{\xi}^{\mathtt{e}}_{\mathtt{g}})\, f\big(\boldsymbol{x}(\boldsymbol{\xi}^{\mathtt{e}}_{\mathtt{g}})\big) w^{\mathtt{e}}_{\mathtt{g}} + \sum_{\partial\Omega_i \cap \Gamma_D} \tau_i \sum_{\mathtt{g}=1}^{\mathtt{n}^{\mathtt{f}}_{\mathtt{ip}}} \mathbf{N}(\boldsymbol{\xi}^{\mathtt{f}}_{\mathtt{g}})\, u_D\big(\boldsymbol{x}(\boldsymbol{\xi}^{\mathtt{e}}_{\mathtt{g}})\big) w^{\mathtt{f}}_{\mathtt{g}},$$

$$[\mathbf{f}_q]_i = \sum_{\partial\Omega_i \cap \Gamma_D} \sum_{\mathtt{g}=1}^{\mathtt{n}^{\mathtt{f}}_{\mathtt{ip}}} \mathbf{N}_{\boldsymbol{n}}(\boldsymbol{\xi}^{\mathtt{f}}_{\mathtt{g}})\, u_D\big(\boldsymbol{x}(\boldsymbol{\xi}^{\mathtt{f}}_{\mathtt{g}})\big) w^{\mathtt{f}}_{\mathtt{g}},$$

$$[\mathbf{A}_{u\hat{u}}]_i = \sum_{\partial\Omega_i \setminus \Gamma_D} \tau_i \sum_{\mathtt{g}=1}^{\mathtt{n}^{\mathtt{f}}_{\mathtt{ip}}} \mathbf{N}(\boldsymbol{\xi}^{\mathtt{f}}_{\mathtt{g}})\, \widehat{\mathbf{N}}^T(\boldsymbol{\xi}^{\mathtt{f}}_{\mathtt{g}}) w^{\mathtt{f}}_{\mathtt{g}},$$

$$[\mathbf{A}_{q\hat{u}}]_i = \sum_{\partial\Omega_i \setminus \Gamma_D} \sum_{\mathtt{g}=1}^{\mathtt{n}^{\mathtt{f}}_{\mathtt{ip}}} \mathbf{N}_{\boldsymbol{n}}(\boldsymbol{\xi}^{\mathtt{f}}_{\mathtt{g}})\, \widehat{\mathbf{N}}^T(\boldsymbol{\xi}^{\mathtt{f}}_{\mathtt{g}}) w^{\mathtt{f}}_{\mathtt{g}},$$

$$[\mathbf{A}_{\hat{u}\hat{u}}]_i = -\sum_{\partial\Omega_i \setminus \Gamma_D} \tau_i \sum_{\mathtt{g}=1}^{\mathtt{n}^{\mathtt{f}}_{\mathtt{ip}}} \widehat{\mathbf{N}}_{\boldsymbol{n}}(\boldsymbol{\xi}^{\mathtt{f}}_{\mathtt{g}})\, \widehat{\mathbf{N}}^T(\boldsymbol{\xi}^{\mathtt{f}}_{\mathtt{g}}) w^{\mathtt{f}}_{\mathtt{g}}$$

and

$$[\mathbf{f}_{\hat{u}}]_i = -\sum_{\partial\Omega_i \cap \Gamma_N} \sum_{\mathtt{g}=1}^{\mathtt{n}^{\mathtt{f}}_{\mathtt{ip}}} \mathbf{N}(\boldsymbol{\xi}^{\mathtt{f}}_{\mathtt{g}})\, t\big(\boldsymbol{x}(\boldsymbol{\xi}^{\mathtt{f}}_{\mathtt{g}})\big) w^{\mathtt{f}}_{\mathtt{g}}.$$

In the above expressions, $\boldsymbol{\xi}^{\mathtt{e}}_{\mathtt{g}}$ and $w^{\mathtt{e}}_{\mathtt{g}}$ are the $\mathtt{n}^{\mathtt{e}}_{\mathtt{ip}}$ integration points and weights defined on the reference element and $\boldsymbol{\xi}^{\mathtt{f}}_{\mathtt{g}}$ and $w^{\mathtt{f}}_{\mathtt{g}}$ are the $\mathtt{n}^{\mathtt{f}}_{\mathtt{ip}}$ integration points and weights defined on the reference edge/face. The implementation considered here adopts the numerical quadratures recently proposed by Witherden and Vincent (2015).

Similarly, the different matrices appearing in (25), computed for each element $i = 1, \ldots, \mathtt{n}_{\mathtt{el}}$, can be expressed as

$$[\mathbf{A}^{\star}_{uu}]_i = \sum_{\partial\Omega_i \setminus \Gamma_N} \tau_i \sum_{\mathtt{g}=1}^{\mathtt{n}^{\mathtt{f}}_{\mathtt{ip}}} \mathbf{N}(\boldsymbol{\xi}^{\mathtt{f}}_{\mathtt{g}})\, \mathbf{N}^T(\boldsymbol{\xi}^{\mathtt{f}}_{\mathtt{g}}) w^{\mathtt{f}}_{\mathtt{g}},$$

Preprint of
Ruben Sevilla and Antonio Huerta. "Tutorial on Hybridizable Discontinuous Galerkin (HDG) for Second-Order Elliptic Problems."
Advanced Finite Element Technologies. Springer International Publishing, 2016. 105-129.

$$[\mathbf{A}^{\star}_{uq}]_i = \sum_{\mathtt{g}=1}^{\mathtt{n}^{\mathtt{e}}_{\mathtt{ip}}} \mathbf{N}(\boldsymbol{\xi}^{\mathtt{e}}_{\mathtt{g}})\, \boldsymbol{\nabla}\mathbf{N}^T(\boldsymbol{\xi}^{\mathtt{e}}_{\mathtt{g}}) w^{\mathtt{e}}_{\mathtt{g}} - \sum_{\partial\Omega_i\cap\Gamma_N} \sum_{\mathtt{g}=1}^{\mathtt{n}^{\mathtt{f}}_{\mathtt{ip}}} \mathbf{N}(\boldsymbol{\xi}^{\mathtt{f}}_{\mathtt{g}})\, \mathbf{N}_{\boldsymbol{n}T}(\boldsymbol{\xi}^{\mathtt{f}}_{\mathtt{g}}) w^{\mathtt{f}}_{\mathtt{g}},$$

$$[\mathbf{f}^{\star}_{u}]_i = \sum_{\mathtt{g}=1}^{\mathtt{n}^{\mathtt{e}}_{\mathtt{ip}}} \mathbf{N}(\boldsymbol{x}^{\mathtt{e}}_{\mathtt{g}})\, f\big(\boldsymbol{x}(\boldsymbol{\xi}^{\mathtt{f}}_{\mathtt{g}})\big) w^{\mathtt{e}}_{\mathtt{g}} + \sum_{\partial\Omega_i\cap\Gamma_N} \sum_{\mathtt{g}=1}^{\mathtt{n}^{\mathtt{f}}_{\mathtt{ip}}} \mathbf{N}(\boldsymbol{x}^{\mathtt{f}}_{\mathtt{g}})\, t\big(\boldsymbol{x}(\boldsymbol{\xi}^{\mathtt{f}}_{\mathtt{g}})\big) w^{\mathtt{f}}_{\mathtt{g}}$$
$$+ \sum_{\partial\Omega_i\cap\Gamma_D} \tau_i \sum_{\mathtt{g}=1}^{\mathtt{n}^{\mathtt{f}}_{\mathtt{ip}}} \mathbf{N}(\boldsymbol{\xi}^{\mathtt{f}}_{\mathtt{g}})\, u_D\big(\boldsymbol{x}(\boldsymbol{\xi}^{\mathtt{f}}_{\mathtt{g}})\big) w^{\mathtt{f}}_{\mathtt{g}},$$

$$[\mathbf{A}^{\star}_{u\hat{u}}]_i = \sum_{\partial\Omega_i\setminus\partial\Omega} \tau_i \sum_{\mathtt{g}=1}^{\mathtt{n}^{\mathtt{f}}_{\mathtt{ip}}} \mathbf{N}(\boldsymbol{\xi}^{\mathtt{f}}_{\mathtt{g}})\, \widehat{\mathbf{N}}^T(\boldsymbol{\xi}^{\mathtt{f}}_{\mathtt{g}}) w^{\mathtt{f}}_{\mathtt{g}},$$

$$[\mathbf{A}^{\star}_{q\hat{u}}]_i = \sum_{\partial\Omega_i\setminus\partial\Omega} \sum_{\mathtt{g}=1}^{\mathtt{n}^{\mathtt{f}}_{\mathtt{ip}}} \mathbf{N}_{\boldsymbol{n}}(\boldsymbol{\xi}^{\mathtt{f}}_{\mathtt{g}})\, \widehat{\mathbf{N}}^T(\boldsymbol{\xi}^{\mathtt{f}}_{\mathtt{g}}) w^{\mathtt{f}}_{\mathtt{g}}$$

and

$$[\mathbf{A}^{\star}_{\hat{u}\hat{u}}]_i = -\sum_{\partial\Omega_i\setminus\partial\Omega} \tau_i \sum_{\mathtt{g}=1}^{\mathtt{n}^{\mathtt{f}}_{\mathtt{ip}}} \widehat{\mathbf{N}}_{\boldsymbol{n}}(\boldsymbol{\xi}^{\mathtt{f}}_{\mathtt{g}})\, \widehat{\mathbf{N}}^T(\boldsymbol{\xi}^{\mathtt{f}}_{\mathtt{g}}) w^{\mathtt{f}}_{\mathtt{g}}.$$